Sensors and Actuators A 156 (2009) 359–365

Contents lists available at ScienceDirect

Sensors and Actuators A: Physical

journal homepage: www.elsevier.com/locate/sna

Cylindrical ultrasonic linear microactuator based on quasi-traveling wave propagation on a thin film metallic glass pipe supported by a piezoelectric ceramic tube

Dongming Sun[a,*], Sheng Wang[a], Seiichi Hata[a,**], Junpei Sakurai[a], Akira Shimokohbe[b]

[a] Precision and Intelligence Laboratory, Tokyo Institute of Technology, 4259 S1-1 Nagatsuta-cho, Midori-ku, Yokohama 226-8503, Japan
[b] Tokyo Institute of Technology, Japan

A R T I C L E I N F O

Article history:
Received 3 October 2008
Received in revised form 2 October 2009
Accepted 8 October 2009
Available online 6 November 2009

Keywords:
Microactuator
Linear
Cylindrical
Ultrasonic
Vibration

A B S T R A C T

A novel ultrasonic linear microactuator with a circular cylindrical stator and slider structure is presented. The stator consists of a cylindrical piezoelectric ceramic tube and an elastic material, a thin film metallic glass (TFMG) pipe. In finite element simulations, a quasi-traveling wave is generated on the TFMG pipe, and trajectories of particles on the pipe are determined to be elliptical motion. There is good agreement between the simulations and measurement results for the vibration of the fabricated stator. Bi-directional motion of the slider is successfully observed at 613 kHz, and the maximum velocity is about 25 mm/s at 30 V.

1. Introduction

Ultrasonic microactuators based on the converse piezoelectric effect in piezoelectric ceramic materials are being rapidly developed because of various advantages of high torque at low speed, quick response, high precision controllability, absence of electromagnetic interference, lightweight, and quiet operation. They could be used for precision positioning and motion control in commercial, military and aerospace applications [1–6]. Thus far, several types of ultrasonic microactuators have been proposed. In the ring type microactuator, a traveling wave is generated based on the degenerate eigenmodes of the ring lead zirconate titanate (PZT) material [7,8]. In the linear type, a standing wave is generated by a combination of eigenmodes or by setting some protuberance on the surface of the PZT material [9,10]. In addition, a traveling wave can also be obtained using an elastic guide beam or surface acoustic waves [11,12]. In recently reported linear type microactuators, the sliders are usually smaller compared to the long stators. Therefore, the energy conversion coefficient is low since the energy is consumed on the long vibration beam [12,13].In this work, a novel cylindrical ultrasonic linear microactuator (CULMA) with bi-directional motion is presented. The CULMA with a compact structure is composed of a stator and slider with similar geometric sizes, which is different from previous devices typically had longer guide beams or larger driving areas [11,12]. In particular, this type of microactuator does not require a guideway mechanism since the cylindrical slider is moving along the stator. Bi-directional motion of the slider is realized based on a traveling wave generated on the stator.

2. Design and fabrication

The stator in the present study consists of a PZT tube and an elastic material, a thin film metallic glass (TFMG) pipe. Metallic glasses are suitable for micromachining, and are an ideal material for microelectromechanical systems (MEMS) because of their favorable characteristics, including mechanical isotropy, thermal stability, structural homogeneity, and absence of crystalline defects [14,15]. In particular, TFMG has a smaller stiffness than other MEMS materials, for example, polysilicon. Since the Young's modulus of TFMG is only half that of polysilicon, TFMG can be used to form micro-elastic structures [16,17].

The structure and basic driving principle of CULMA are illustrated in the sectional view in Fig. 1. The TFMG pipe with an expansion region in the middle is fabricated on a PZT tube, which is polarized in the radial (r) direction. The PZT tube vibrates based on the converse piezoelectric effect under a high frequency harmonic voltage applied on the inner and outer electrodes of the

* Corresponding author. Tel.: +81 45 924 5745.
** Corresponding author.
E-mail addresses: dongming.sun.01@gmail.com (D. Sun), shata@pi.titech.ac.jp (S. Hata).

0924-4247/$ – see front matter © 2009 Elsevier B.V. All rights reserved.
doi:10.1016/j.sna.2009.10.004

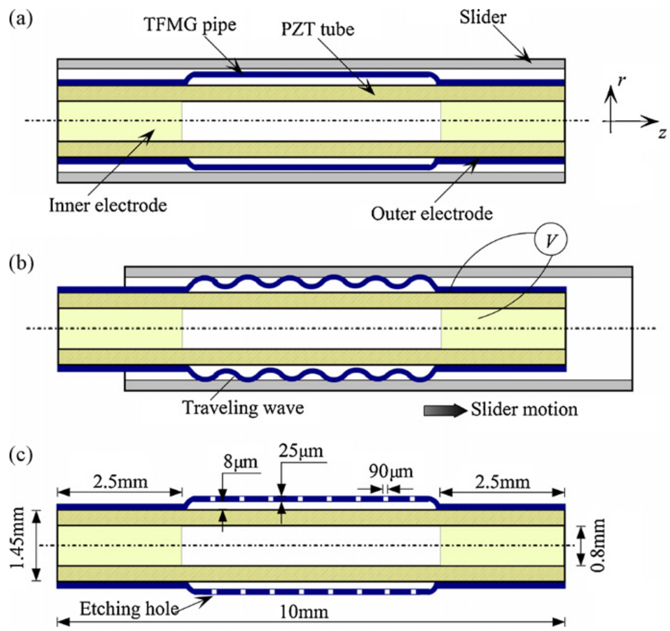

Fig. 1. Section view of the basic principle of the CULMA (a and b) and the geometrical structure of the stator (c).

PZT tube. The TFMG pipe usually vibrates as a standing wave at its eigenmode under the excitation of the PZT vibration. At some specific frequency and under suitable boundary conditions, however, a traveling wave is generated on the TFMG pipe to drive the slider, which is a precise stainless steel pipe, to move in two directions by changing the voltage signal. Actually, the motion of the traveling wave is considered to be a result of the vibration combination of the PZT tube and the TFMG pipe. The geometrical parameters used are listed in Table 1 and the material properties are listed in Table 2.

Scanning electron microscope (SEM) images of the fabricated stator are shown in Fig. 2. In the fabrication process of the stator, several key techniques are used, including rotating magnetron sputtering, wet-etching, and micro-electrical discharge machining (micro-EDM). A sacrificial layer of Al is deposited on the center part of the PZT tube using the rotating RF-magnetron sputtering system, with a deposition rate of ∼24 nm/min. The TFMG, with a composition of $Pd_{76}Cu_6Si_{18}$ (at.%), is then deposited with a rate of ∼38 nm/min. On the expansion region of the TFMG pipe, etching holes are formed using micro-EDM. The sacrificial layer (Al) is etched through the etching holes using a solution of tetramethylammonium hydroxide (TMAH). After cleaning and baking treatments, the stator is then ready to be measured.

Table 1
Geometrical parameters of the stator.

Geometrical parameter	Variable	Value (unit)
Length of PZT	L	10 (mm)
Length of electrode	L_E	2.5 (mm)
Inner diameter of PZT	r_{PZT}	800 (μm)
Thickness of PZT	w_{PZT}	325 (μm)
Length of TFMG pipe	l	5 (mm)
Thickness of TFMG pipe	w	25 (μm)
Inner diameter of TFMG pipe	r	1466 (μm)
Gap between PZT and TFMG pipe	Δr	8 (μm)

3. Analysis and finite element method (FEM) simulation

The vibration characteristics of the PZT tube and the TFMG pipe have a special reference to design the CULMA. The driving effect of the stator is a combination of the axial vibration of the PZT tube and radial vibration of the TFMG pipe. Analytical calculation and FEM simulation are two methodologies used, and the results are compared in the following discussion.

For the PZT tube, we utilized the Haskins and Walsh model [18–20] to calculate the axial eigenmodes. The relationship between the frequency f and the length of the PZT tube from the first to sixth modes is shown in Fig. 3; the solid line represents the analytical solutions and the square symbol line represents the FEM simulation results. The boundary conditions of the PZT tube are set as 'simply supported'. Basically, the two results are in a good agreement except for the region at the top left corner in the figure, where there are some deviations for the smaller length and higher frequency. The frequency of 800 kHz is close to the radial vibration frequency of the PZT tube, and strong coupling vibration of radial and longitudinal directions occurs, therefore the analytical solutions might have some errors in this region. The dashed line denotes the situation where the length equals 10 mm, and the first

Table 2
Material properties of TFMG and PZT.

Variable	Material property	Value (unit)
ρ	Density of TFMG	10.42×10^3 (kg/m^3)
ρ_{PZT}	Density of PZT	7.7×10^3 (kg/m^3)
σ	Poisson's ratio of TFMG	0.33
σ_{PZT}	Poisson's ratio of PZT	0.34
$\tan\delta$	Dissipation factor of TFMG	0.15 (%)
$\tan\delta'$	Dissipation factor of PZT	1.5 (%)
E	Young's modulus of TFMG	88 (GPa)
s^E	Elastic compliance constants of PZT	$\begin{vmatrix} 1.69 & -0.58 & -0.62 & 0 & 0 & 0 \\ -0.58 & 1.69 & -0.62 & 0 & 0 & 0 \\ -0.62 & -0.62 & 1.96 & 0 & 0 & 0 \\ 0 & 0 & 0 & 5.0 & 0 & 0 \\ 0 & 0 & 0 & 0 & 5.0 & 0 \\ 0 & 0 & 0 & 0 & 0 & 4.54 \end{vmatrix} \times 10^{-11}$(1/Pa)
d	Piezoelectric charge constants of PZT	$\begin{vmatrix} 0 & 0 & 0 & 0 & 670 & 0 \\ 0 & 0 & 0 & 670 & 0 & 0 \\ -185 & -185 & 435 & 0 & 0 & 0 \end{vmatrix} \times 10^{-12}$(C/N)
ε^T	Relative permittivity constants of PZT	$\begin{vmatrix} 1960 & 0 & 0 \\ 0 & 1960 & 0 \\ 0 & 0 & 1850 \end{vmatrix}$
T_c	Curie point of PZT	345 (°C)
Q_m	Mechanical quality factor of PZT	80